Transition Met Chem (2011) 36:669–677
DOI 10.1007/s11243-011-9517-8

Binuclear vanadium(V) complexes of bis(aryl)adipohydrazone: synthesis, spectroscopic studies, crystal structure and catalytic activity

**Nasim Asghari Lalami · Hassan Hosseini Monfared ·
Hashem Noei · Peter Mayer**

Received: 19 May 2011 / Accepted: 7 July 2011 / Published online: 29 July 2011

Abstract Three new binuclear vanadium(V) complexes of bis(aryl)adipohydrazones (H_4L^1 = bis((2-hydroxynaphthalen-1-yl)methylene)adipohydrazide, H_4L^2 = bis(5-bromo-2-hydroxybenzylidene)adipohydrazide, and H_4L^3 = bis(2-hydroxy-3-methoxybenzylidene)adipohydrazide) were synthesized by direct reaction of [VO(acac)$_2$] with the hydrazone ligands. The ligands and complexes were characterized by FT–IR, UV–Vis, and NMR spectroscopic methods. The crystal structures of the complexes of L^1 and L^3 were determined by X-ray analyses. The solid-state structure of the complex of L^1 features a 1D hydrogen-bonded chain from N···H–O hydrogen bonding. The catalytic activities of these complexes have been tested in the oxidation of various hydrocarbons using H_2O_2 as the terminal oxidant. Generally, good to excellent conversions have been obtained.

Introduction

Hydrazones, especially acyl and aroyl hydrazones, are a multipurpose class of ligands having a range of biological and chemical activities. Hydrazones exhibit physiological and biological activities in the treatment of several diseases such as tuberculosis [1], for the treatment of Fe overload disease [2–4], and as inhibitors for many enzymes [5]. These properties of the hydrazones are attributed to the formation of stable chelate complexes with transition metals that catalyze physiological processes. Their metal complexes have also found applications in various chemical processes like non-linear optics, sensors, and medicine [6]. They are of interest in the field of electrochromism where a change in the oxidation state of the metal is possible [7, 8]. Aroylhydrazone complexes, on the other hand, seem to be a good candidate for catalytic oxidation studies because of their stability towards oxidation. Acyl and aroyl hydrazones –CO–NH–N=CRR′ (R and R′=H, alkyl, aryl) contain trigonal N- and O-donor atoms that can coordinate to metal ions [9, 10]. Hydrazone ligands can act as bidentate, tridentate, or tetradentate ligands depending on the nature of heterocyclic ring substituents attached to the hydrazone unit. These ligands due to their facile keto–enol tautomerization and the availability of several potential donor sites can coordinate with metals. In the field of hydrazone chemistry, the study of bis(aryl)hydrazone complexes is of interest for several reasons: (1) the study of the bis(aryl)hydrazone complexes is justified by the presence of two hydrazone coordinating units in ditopic ligands, which may yield supramolecular architectures or coordination polymers [11], (2) the coordination of a metal ion by one unit may induce changes in the coordinative properties of the other unit, and (3) binuclear complexes of these ligands are suitable for weak spin–spin exchange interactions studies [12].

The coordination chemistry of vanadium containing VO^{2+} or VO^{3+} moieties has received considerable attention probably due to their association in many vanadium-dependent enzymes,

---

Electronic supplementary material The online version of this article (doi:10.1007/s11243-011-9517-8) contains supplementary material, which is available to authorized users.

N. Asghari Lalami · H. Hosseini Monfared (✉) · H. Noei
Department of Chemistry, Zanjan University, 45195-313 Zanjan, Islamic Republic of Iran
e-mail: monfared@znu.ac.ir; monfared_2@yahoo.com
URL: http://www.znu.ac.ir/members/hosseini_hassan

P. Mayer
Fakultät für Chemie und Pharmazie, Ludwig-Maximilians-Universität, München, Butenandtstr. 5-13, Haus D,
81377 München, Germany

such as nitrogenases [13], haloperoxidases [14], phosphomutases [15], and nitrate reductases [16]. Functional model compounds have been developed by studies in structures, chemical, and medical properties of these vanadium enzymes [13, 17]. Hydrazides and hydrazones have interesting ligation properties due to the presence of several coordination sites, and these ligands have a tendency to stabilize the vanadium in its highest oxidation state [18, 19]. Vanadium compounds have been widely used as catalysts in peroxidic as well as dioxygenic oxidation of hydrocarbons [20, 21], but so far yields and turnover number obtained are not very remarkable [22].

Because of the importance of vanadium complexes, and as a part of our search in the study of coordinating capabilities of aroyl hydrazones and their coordination compounds, we are extending our research on the efficacious compounds of binuclear vanadium. Here, we report the synthesis, characterization, and catalytic activity (as modeling the haloperoxidase activity) of binuclear oxovanadium(V) complexes of bis(aryl)hydrazone ligands H_4L^1, H_4L^2, and H_4L^3 derived from 2-hydroxynaphtaldehyde/adipichydrazide, 3-bromosalicylaldehyde/adipichydrazide, and 3-methoxysalicylaldehyde/adipichydrazide, respectively (Scheme 1). The crystal structures of two of these vanadium complexes were also determined.

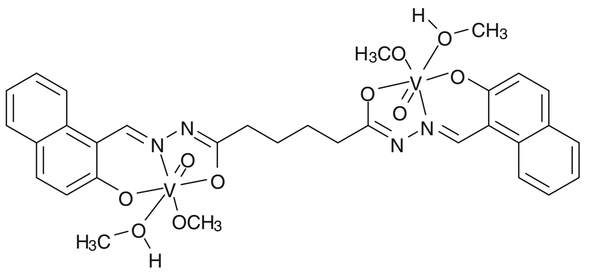

$[\{VO(CH_3OH)(OCH_3)\}_2L^1]$, **1**

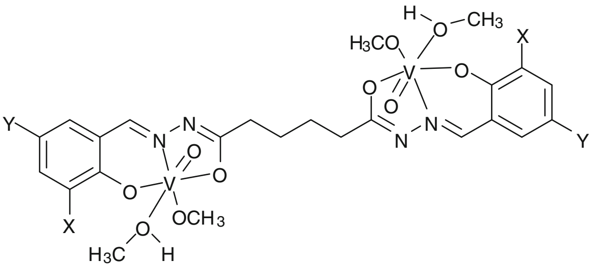

$[\{VO(CH_3OH)(OCH_3)\}_2L^2]$, **2** :X=H, Y=Br
$[\{VO(CH_3OH)(OCH_3)\}_2L^3]$.2CH3OH, **3** :X=OCH3, Y=H

Scheme 1 The synthesized hexadentate adipichydrazone-vanadium(V) complexes

Results and discussion

The bis(aryl)adipohydrazone ligands (H_4L^1, H_4L^2, and H_4L^3) were synthesized in high yield and excellent purity by condensation reaction of adipohydrazide with 2 equivalents of the corresponding arylaldehydes (2-hydroxynaphthaldehyde, bromosalicylaldehyde, and 3-methoxy salicylaldehyde). Ligands H_4L^{1-3} react with $[VO(acac)_2]$ to give binuclear metal complexes of formulae $[\{VO(CH_3OH)(OCH_3)\}_2L^1]$ (**1**), $[\{VO(CH_3OH)(OCH_3)\}_2L^2]$ (**2**) and $[\{VO(CH_3OH)(OCH_3)\}_2L^3]\cdot 2CH_3OH$ (**3**) (Scheme 1).

Spectroscopic characterization

A list of IR spectral data is presented in Table 1. A comparison of the spectra of the complexes with the ligands provides evidence for the coordination mode of the ligands in the complexes. The non-observation of the ν(C=O) bands, present in the ligands at 1,658–1,668 cm^{-1}, indicates the enolization of the amide functionality upon coordination to the V^V-center. Instead, strong bands at ca. 1,602–1,617 cm^{-1} are observed, which can be attributed to the asymmetric stretching vibration of the conjugated CH=N–N=C group [23], characteristic of the coordination of the enolate form of the ligands.

On complexation, the absence of N–H band and red-shifts in azomethine (–C=N–) band of the ligands show coordination of H_4L^{1-3} as tetraianionic ligands in enol form through the deprotonated hydroxyl group ($O_{phenolate}$), azomethine nitrogen ($N_{azomethine}$), and enol oxygen groups ($O_{O\text{–}C(naphthyl)=N}$) in the complexes **1**, **2**, **3** (Table 1). A strong C=N stretch (around 1,610 cm^{-1}) indicates the C=N group of the coordinated Schiff base ligands [24]. The strong ν(VO) band around 990 cm^{-1} could be clearly identified for all the complexes.

H_4L^1, H_4L^2, and H_4L^3 were soluble in polar and common organic solvents like methanol and formed green, white-cream, and cream solutions, respectively. These solutions have been used to record the electronic spectra.

Table 1 IR spectral data of the ligands and the vanadium complexes

Selected IR bands (cm^{-1})					
Compound	ν(C=N)[a] + δ(NH)	ν(C=O)	ν(NH)	ν(OH)	ν(V=O)
H_4L^1	1,624, 1,599	1,658	3,196	3,463	
H_4L^2	1,617, 1,544	1,677	3,275	3,431	
H_4L^3	1,631, 1,579	1,668	3,215	3,454	
	ν(C=N–N=C)				
1	1,602				994
2	1,617				983
3	1,610				999

[a] The bands assigned to ν(C=N) (azomethine) may not be pure, as they may be associated with the aromatic (C=C) stretching bands

Table 2 ^1H NMR of ligands H_4L^1–H_4L^3

Compound	Solvent	–CO–CH_2	–CH=N–	NH	–OH
H_4L^1	$(CD_3)_2SO$	2.30, 2.65	8.90, 9.15	11.23, 11.66	12.63
H_4L^1	$(CD_3)_2SO + D_2O$	2.30, 2.63	8.87, 9.10	–	–
Complex **1**	$(CD_3)_2SO$	1.73, 2.05	9.60	–	–
H_4L^2	$(CD_3)_2SO$	2.22, 2.60	8.10, 8.20	10.26, 11.10	11.17, 11.58
H_4L^2	$(CD_3)_2SO + D_2O$	2.45	8.31	–	–
H_4L^3	$(CD_3)_2SO$	2.22, 2.58	8.20, 8.30	9.48, 10.86	11.15, 11.50
H_4L^3	$(CD_3)_2SO + D_2O$	2.20, 2.55	8.30, 8.25	–	–

The hydrazone ligands showed three bands in the range 200–800 nm (Fig. S1). Based on their extinction coefficients and energies, these are assigned to $\pi \rightarrow \pi^*$ (227–237 nm bands), $\pi \rightarrow \pi^*$ and $n \rightarrow \pi^*$ (282–320 nm bands), and $n \rightarrow \pi^*$ (331–370 nm) transitions. The dark brown complexes **1–3** were not soluble in polar or non-polar solvents; therefore, their UV–Vis spectra could not be recorded in solution.

^1H NMR data of the ligands and the complex **1** are given in Sect. 2 and Table 2. On the basis of intensity, chemical shift values, and deutration experiments, we assigned the signals. In all the three ligands, two groups of methylene next to carbonyl, azomethine, and NH are not equivalent and gave different signals (Table 2). Aromatic protons of the ligands appear well within the expected range (6.55–7.70 ppm). The azomethine group –CH=N that is formed in the condensation reaction in H_4L^{1-3} showed singlet signals in the range 8.10–9.15 ppm. The NH and OH groups of the ligands H_4L^2 and H_4L^3 have signals about 9.48–11.10 and 11.15–11.58 ppm (in DMSO-d^6), respectively. These signals disappear in the presence of D_2O. The chemical shifts for NH (11.23, 11.66) and OH (12.63) groups of H_4L^1 are higher than the corresponding groups in H_4L^2 and H_4L^3. While complexes **2** and **3** were not soluble in DMSO, D_2O, and $CDCl_3$, complex **1** was slightly soluble in DMSO. The absence of NH and OH signals in the ^1H NMR spectrum of **1** confirmed the coordination of the tetra-deprotonated ligand $(L^1)^{4-}$ in enol form through phenolate oxygen ($O_{phenolate}$) and enol oxygen atoms ($O_{O-C(naphthyl)=N}$) to V(V).

X-ray structures of $[\{VO(CH_3OH)(OCH_3)\}_2L^1]$ (**1**) and $[\{VO(CH_3OH)(OCH_3)\}_2L^3]\cdot 2CH_3OH$(**3**)

The molecular structures and labeling of the atoms for complexes **1** and **3** are displayed in Figs. 1 and 2, and selected bond lengths and angles are given in Table 3. There are two non-coordinated methanol molecules present in **3**.

Since structural analyses show that compounds **1** and **3** are both binuclear vanadium compounds and contain the similar building unit $[\{VO(CH_3OH)(OCH_3)\}_2L]$, compound **1** is selected to represent their structures. Compounds **1** and **3** are binuclear centrosymmetric compounds. The two dianionic, tridentate domains of the ligand adopt a trans configuration, and each coordinates a V(V) ion forming a dimetal complex. In **1**, vanadium adopts a distorted octahedral coordination geometry with two oxygen atoms and one nitrogen atom (O1, O2, and N2) from L ligand with an oxygen atom (O5) of methoxylate occupying an equatorial position and two oxygen atoms occupying two axial positions, where one oxygen (O3) is terminal and the other (O4) is from methanol. The axial V=O bond distance of the terminal oxygen 1.586(3) Å in **1** is 0.17 Å shorter than those of the equatorial oxygen atoms (1.756(3)–1.957(3) Å), while the other axial V–O bond (2.304(3) Å) is significantly longer than the equatorial V–O bonds due to the trans effect of V=O bond. The V=O distance

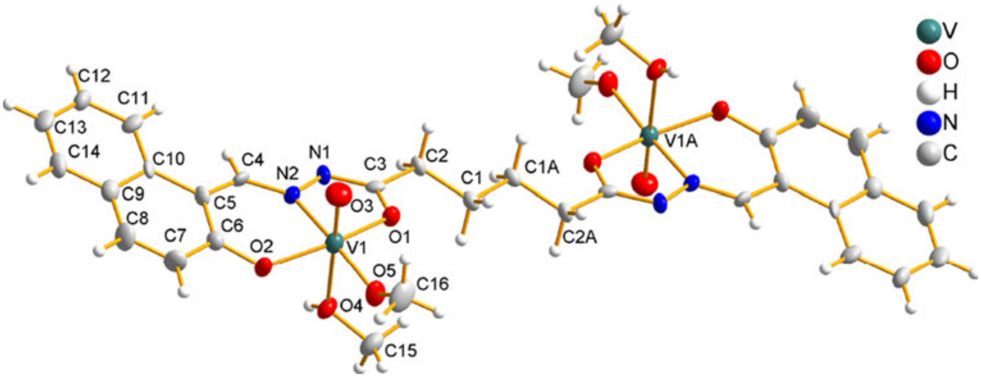

Fig. 1 Thermal ellipsoid plot (50% probability) of the repeat unit in $[\{VO(CH_3OH)(OCH_3)\}_2L^1]$ (**1**); bond lengths and angles are provided in Table 3; symmetry transformations A = 2−x, −y, −z. Only one of two symmetry-independent halves of molecules is shown in the figure. Non-labeled non-hydrogen atoms are generated by symmetry operation A

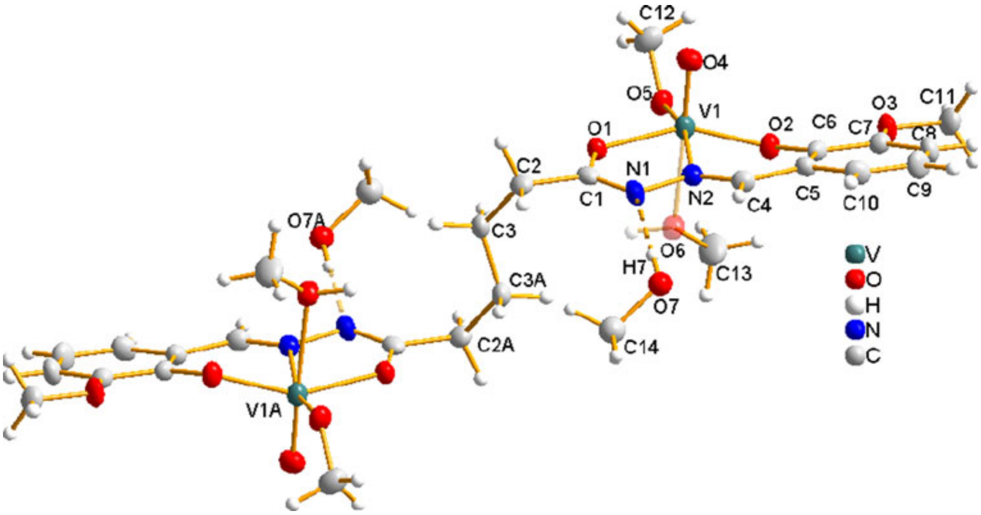

Fig. 2 Thermal ellipsoid plot (50% probability) of the repeat unit in $[\{VO(CH_3OH)(OCH_3)\}_2L^3]\cdot 2CH_3OH$ (**3**), bond lengths and angles are given in Table 3; symmetry transformations A = −x, 1−y, −z. Non-labeled non-hydrogen atoms are generated by symmetry operation A

Table 3 Selected bond distances (Å) and angels (deg) for complexes **1** and **3**

Complex **1**		Complex **3**	
V1–O1	1.957(3)	V1–O1	1.9,786(19)
V1–O2	1.862(3)	V1–O2	1.8523(18)
V1–O3	1.586(2)	V1–O4	1.596(2)
V1–O4	2.304(3)	V1–O5	1.776(2)
V1–O5	1.756(3)	V1–N2	2.116(2)
V1–N2	2.102(3)	V1–O6	2.295(2)
O1–V1–O2	151.76(12)	O1–V1–O2	151.60(9)
O1–V1–O3	98.41(13)	O1–V1–O4	98.48(10)
O1–V1–O4	80.19(10)	O1–V1–O5	93.83(9)
O1–V1–O5	95.62(12)	O1–V1–O6	78.06(8)
O1–V1– N2	74.54(12)	O1–V1–N2	74.20(9)
O2–V1–O3	99.44(14)	O2–V1–O4	99.89(10)
O2–V1–O4	81.06(11)	O2–V1–O5	103.73(9)
O2–V1–N2	82.08(12)	O2–V1–O6	81.70(8)
O2–V1–O5	101.92(12)	O2–V1–N2	83.96(9)
O3–V1–O4	177.44(14)	O4–V1–N2	91.09(10)
O3–V1–N2	95.61(14)	O4–V1–O5	100.79(11)
O3–V1–O5	101.78(13)	O4–V1–O6	174.23(9)
O4–V1–N2	81.95(11)	O5–V1–N2	164.36(9)
O4–V1–O5	80.55(11)	O5–V1–O6	84.14(8)
O5–V1–N2	161.18(13)	O6–V1–N2	83.54(8)

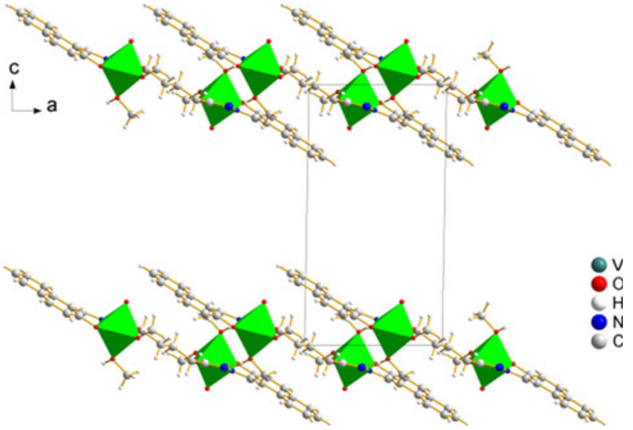

Fig. 3 Infinite supramolecular chains along [100] in **1** established by hydrogen bonds of the typeN···H–O

in complex **1** (1.586 Å) and **3** (1.5,957 Å) are close to another reported complex [25]. The larger V–O4 bond distance indicates a markedly weaker coordination of the axial methanol molecule. The L anion bridges two vanadium ions. The deprotonated bis(aryl)adipohydrazone ligand forms an equatorial plane (O1, N2, O2, O5 for molecule **1**) through the naphtholate oxygen atom O2, imine nitrogen atom N2, and enolate oxygen atom O1 together with the oxygen atom O5 from the methoxylate ligand. Relative to this plane, the vanadium atom is displaced toward the terminal oxygen atom O3 by 0.30 Å in complex **1**. C1, C2, and the atoms of the naphthyl units are almost coplanar with the mean deviation from the plane 0.144–0.163 Å. The coordinating atom plane (O1/N2/O2/O5) makes a dihedral angle of 16.65° with the naphthyl plane.

The binuclear entities of **1** form a supramolecular 1D chain as a result of two hydrogen bonds of the type N···H–O (Fig. 3, Table 4). In **3**, each dinuclear complex is linked to four adjacent complexes through hydrogen bonds involving either methanol atoms (Fig. 3).

Catalytic reactivity

The catalytic oxidation of cyclooctene as a representative substrate with hydrogen peroxide was studied in the presence of complexes **1**, **2**, and **3**. The results of control experiments revealed that the presence of catalyst and

Table 4 Hydrogen bonding interaction in **1** and **3**

Complex	D–H···A (Å)	D–H (Å)	H···A (Å)	D···A (Å)	D–H···A (deg)
1	O4–H4···N1[1]	0.90(2)	1.87(2)	2.761(4)	168(3)
	O10–H10···N3[2]	0.84(3)	1.90(3)	2.726(4)	166(3)
3	O6–H6···O7[3]	0.96	1.79	2.723(3)	163.4
	O7–H7···N1	0.91	1.87	2.782(3)	177.1

D Donor, *A* acceptor

SD are given in parentheses

Symmetry transformation: [1] 1−*x*, −*y*, −*z*; [2] 1−*x*, −*y*, 1−*z*; [3] *x*, 1/2−y, −1/2 + *z*

Table 5 Catalytic epoxidation of cyclooctene with H_2O_2 in CH_3CN

Entry	Catalyst	Yield (%)[a]	Time (h)
1	**1**	22 (53)[b]	1 (5)
2	**2**	33 (62)[b]	1 (5)
3	**3**	58 (97)[b]	1 (3)

Reaction conditions: catalyst, 1.3 μmol; cyclooctene, 1 mmol; internal standard (chlorobenzene), 0.1 g; CH_3CN, 3 mL; H_2O_2, 3 mmol; and reaction temperature, 80 °C

[a] Yields are based on the starting cyclooctene

[b] The number in the bracket refer to the yield after the second time

oxidant (H_2O_2) is essential for the oxidation. Results of the studies are summarized in Table 5. Cyclooctene was converted to the corresponding epoxide with 100% selectivity by all three complexes. The catalyst **3** showed the highest activity (yield 97% after 3 h), followed by **2** (yield 62% after 5 h), and the catalyst **1** showed the least reactivity.

Other parameters for suitable reaction conditions to achieve the maximum oxidation of cyclooctene such as the oxidant concentration (moles of oxidant per moles of cyclooctene), solvent, and temperature of the reaction were investigated. The effect of oxidant concentration on the oxidation of cyclooctene by **3** is illustrated in Table 6, entries 1–3. Different oxidant/cyclooctene molar ratios (1:1, 2:1, and 3:1) were considered while the ratio of cyclooctene (1.0 mmol) to catalyst (1.3 μmol) in 3 mL of acetonitrile at 80 ± 1 °C was constant. The conversion of cyclooctene increased with increasing the amount of hydrogen peroxide in the reaction mixture. When H_2O_2/substrate mole ratio was 3, the maximum conversion of 97% was obtained, showing that about 2 equivalents of the oxidant are decomposed in the non-productive way. This is, however, much less than the decomposition of hydrogen peroxide by bare transition metals [26]. Aqueous hydrogen peroxide was selected by considering its high selectivity, atom economy, and environmentally benign properties.

Table 6 also illustrates the influence of the solvent nature in the catalytic oxidation of cyclooctene by **3**. Methanol, dichloromethane, acetonitrile, and chloroform were used as solvents. Of the various solvents examined, acetonitrile was found to be the most suitable solvent for the reaction. The highest conversion of 97% was obtained in acetonitrile after 3 h. It was observed that the catalytic activity of the catalyst **3** decreased with respect to acetonitrile (relative dielectric constant $\varepsilon/\varepsilon_0$=36, donor number DN = 14.1 [27]) > methanol ($\varepsilon/\varepsilon_0 = 32.6$, DN = 20) > chloroform ($\varepsilon/\varepsilon_0 = 4.8$) ≈ dichloromethane. Overall, the reactivity of catalyst **3** in other solvents was very much lower than acetonitrile (Table 6, entries 3–6). From Table 6, one could see that solvents with moderate donation ability and high polarities seemed to favor this reaction. Solvents with high coordinating property such as methanol (DN = 20) inhibited this reaction.

Table 6 Catalytic epoxidation of cyclooctene with **3**/H_2O_2

Entry	H_2O_2 (mmol)	Solvent	Temp. (°C)	Yield (%)[a]	Time (h)
1	1	CH_3CN	80	3 (43)	1 (5)
2	2	CH_3CN	80	44 (75)	1 (5)
3	3	CH_3CN	80	58 (97)	1 (3)
4	3	CH_3OH	80	0 (30)	1 (5)
5	3	$CHCl_3$	80	0 (0)	1 (5)
6	3	CH_2Cl_2	80	0 (0)	1 (5)
7	3	CH_3CN	60	40 (88)	1 (5)

Reaction conditions: catalyst (**3**), 1.3 μmol; cyclooctene, 1 mmol; internal standard (chlorobenzene), 0.1 g; and solvent, 3 mL

[a] Yields are based on the starting cyclooctene

The cyclooctene yield decreased when the reaction was carried out at lower temperature, 60 °C. With **3** as catalyst, a yield of 88% was obtained after 5 h at 60 °C (Table 6, entry 7), which was lower than the yield 97% at 80 °C.

The catalytic activities of **1–3** were examined in the oxidation of some hydrocarbons in optimized conditions (Table 6) that were proved to be the best for cyclooctene oxidation, and the results are summarized in Tables 7 and 8. Cyclooctene was converted to the corresponding epoxide with 100% selectivity with catalyst **1–3**. But in oxidation of cyclohexene by **3** in addition to cyclohexene oxide (yield

Table 7 Oxidation of various hydrocarbons with $[\{VO(CH_3OH)(OCH_3)\}_2L^3]\cdot 2CH_3OH$ (**3**) using H_2O_2 and acetonitrile

Entry	Substrate	Product(s)	Yield (%)[a]	Selectivity (%)	Conv. (%)[a] (time/h)	TON[b]
1	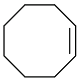	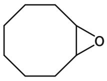	97	100	97 (3)	373
2	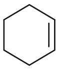	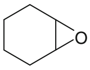	21	22	96 (3)	369
		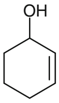	53	55		
		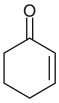	22	23		
3	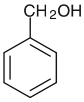	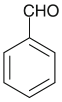	60	100	60 (5)	231
4	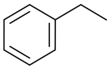	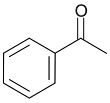	41	100	41 (4)	158
5	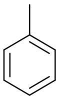	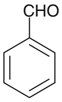	18	100	18 (5)	69

Reaction conditions: catalyst, 1.3 μmol; substrate, 1 mmol; chlorobenzene, 0.1 g; acetonitrile, 3 mL; H_2O_2, 3 mmol; and temperature, 80 ± 1 °C

[a] Yields and conversions are based on the starting substrate and determined by GC

[b] *TON* turnover number = number of moles of product formed per mole of V in the catalyst

Table 8 Comparison of catalytic activities of catalysts **1–3** in the oxidation of various hydrocarbons with hydrogen peroxide

	TOF (h^{-1})[a]		
Substrate	Catalyst **1**	Catalyst **2**	Catalyst **3**
Cyclooctene	74	54	124
Cyclohexene	63	91	123
Benzylalcohol	31	33	46
Ethyl benzene	12	0	40
Toluene	0	0	14

For reaction conditions, see Table 6; in the oxidations with catalysts **1** and **2**, $NaHCO_3$ (0.25 mmol) was used as a co-catalyst to obtain maximum conversion

[a] *TOF* turnover frequency = the catalytic turnover per unit time

21%), also two other products were formed, namely 2-cyclohexene-1-ol (yield 53%) and 2-cyclohexene-1-one (yield 22%). Cyclohexene is more prone to both epoxidation and allylic oxidation [28]. Allylic oxidation has been reported in the metalloporphyrin systems [31] in the oxidation of alkenes such as cyclohexene and reflects the radical nature of the active oxidizing species.

Catalysts **1–3** were also tested in oxidation of benzylalcohol and aromatic compounds (ethylbenzene and toluene). Complex **3** showed the potential to oxidize the side chain of the unreactive aromatic toluene and ethyl benzene to benzaldehyde and acetophenone, respectively, with 100% selectivity and in reasonable yield. Electron-rich alkenes (cyclohexene and cyclooctene) displayed a greater activity than aromatic compounds (benzylalcohol, toluene, and ethylbenzene).

Catalytic activities of three catalysts **1–3** in the oxidation of various hydrocarbons are compared in Table 8. Catalyst **3** is more efficient than **1** and **2**. In addition to solubility differences between the catalysts, there are some electronic and steric differences in the corresponding ligands of the complexes. One could conclude that the presence of electron donor OCH_3 group on the phenolate unit of L^3 improves the catalytic activity of **3** relative to **1** and **2**. The presence of electron withdrawing groups (aryl in **1** and Br in **2**) on the phenolate unit of L^1 and L^2 makes catalysts **1** and **2** less reactive than **3**. These findings are in contrast to our previous studies with mononuclear V(V)=O complexes that proved there was no significant difference in activities between similar structure catalysts [29, 30]. Conclusive interpretation of this subject needs further studies in the future.

The exact mechanism of the reaction is not fully clear. However, on the basis of the oxidation products of the various hydrocarbons (Table 8), it is predicted that the oxidation reactions proceed by intermediacy of a peroxovanadium-hydrazone Schiff base species formed in the reaction mixture in the presence of hydrogen peroxide [29].

Conclusion

Three new binuclear vanadium(V) complexes of bis(aryl) adipohydrazones were synthesized and characterized by spectroscopic methods. The crystal structures of two of the complexes were determined by X-ray analyses. The presence of two hydrazone coordinating units in ditopic ligands yields 1D supramolecular architecture in the complex **1**. The catalytic activities of these complexes have been explored in the oxidation of various hydrocarbons using H_2O_2 as the terminal oxidant. Generally, good to excellent conversions have been obtained.

Experimental

2-hydroxynaphthaldehyde, 3-bromosalicylaldehyde, 3-methoxysalicylaldehyde, adipichydrazide, bis(acetylacetonato)oxovanadium(IV), $[VO(acac)_2]$, and other materials with high purity were purchased from Merck and Fluka and used as received. IR spectra were recorded as KBr disks with a Matson 1000 FT–IR spectrophotometer in the range of 4,000–450 cm^{-1}. UV–Vis spectra in solution were recorded on a Shimadzu 160 spectrometer. ^1H and ^{13}C NMR spectra in DMSO-d^6 solution were recorded on a Bruker 250.13 MHz spectrometer, and chemical shifts are indicated in ppm relative to tetramethylsilane. The reaction products of oxidation were determined and analyzed by HP Agilent 6890 gas chromatograph equipped with a HP-5 capillary column (phenyl methyl siloxane 30 m × 320 μm × 0.25 μm). The elemental analyses (carbon, hydrogen, and nitrogen) were obtained with a Carlo ERBA Model EA 1108 analyzer. Vanadium percentages of complexes were measured by a Varian spectrometer AAS-110.

Synthesis of H_4L^{1-3}

All the three hydrazone ligands (H_4L^{1-3}) were synthesized by the same general method. To a methanol solution (15 mL) of adipichydrazide (0.5 mmol), the appropriate aldehyde (2-hydroxy naphthaldehyde, 5-bromo-2-hydroxybenzaldehyde or 2-hydroxy-3-methoxybenzaldehyde) (1.0 mmol) was added and the mixture refluxed for 5 h. The resulting precipitate was filtered off, washed with methanol, and dried in air**.** NMR data show that each ligand is probably in two forms or is composed of two isomers (isomer I + isomer II).

(N’^{1}E,N’^{6}E)-N’^{1},N’^{6}-bis((2-hydroxynaphthalen-1-yl)methylene)adipohydrazide (H_4L^1)

Yield: 95%. Anal. Calc. for $C_{28}H_{26}N_4O_4$ (MW 482.53): C, 69.7; H, 5.4; N, 11.6. Found: C, 69.8; H, 5.5; N, 11.6. IR (KBr, cm^{-1}): 3,463 (w, O–H), 3,196 (m, N–H), 3,049 (m), 2,947 (m), 1,658 (vs, C=O), 1,624 (s, C=N), 1,599 (w), 1,575 (w), 1,555 (w), 1,469 (s), 1,418 (w0, 1,395 (w), 1,321 (w), 1,284 (w), 1,243 (m), 1,144 (m), 819 (w), 748 (m). ^1H NMR (250.13 MHz, DMSO-d^6, ppm): 1.00 (m, 2H, CH_2), 1.68 (m, 2H, CH_2), 2.30 (m, 2H, CO–CH_2), 2.65 (m, 2H, CO–CH_2), 7.15–8.35 (m, 12H, aryl), 8.90 (s, 1H, CH=N), 9.15 (s, 1H, CH=N), 11.23 (s, 1H, amid N–H), 11.66 (s, 1H, N–H), 12.63 (s, 2H, O–H). UV–Vis spectrum in CH_3OH [λ_{max} (ε, $dm^3\ mol^{-1}\ cm^{-1}$)]: 237 (151,600), 257 (97,400), 312 (48,200), 323 (61,700), 371 nm (47,000).

(N’^{1}E,N’^{6}E)–N’^{1},N’^{6}-bis(5-bromo-2-hydroxybenzylidene)adipohydrazide (H_4L^2)

Yield: 92%. Anal. Calc. for $C_{20}H_{20}Br_2N_4O_4$ (MW 540.21): C, 44.5; H, 3.7; N, 10.4. Found: C, 44.4; H, 3.8; N, 10.4. IR (KBr, cm^{-1}): 3,431 (m, br, O–H), 3,275 (m, N–H), 3,069 (w), 2,958 (w), 1,677 (vs, C=O), 1,617 (s, C=N), 1,544 (m), 1,478 (vs), 1,350 (m), 1,276 (vs), 1,193 (s), 1,141 (w), 979 (w), 700(m), 628 (w). ^1H NMR (250.13 MHz, DMSO-d^6, ppm): 1.59 (m, 4H, CH_2), 2.22 (m, 2H, CO–CH_2), 2.60 (m, 2H, CO–CH_2), 6.55–7.70 (m, 6H, aryl), 8.10 (s, 1H, CH=N), 8.20 (s, 1H, CH=N), 10.26 (s, 1H, amid NH), 11.10 (s, 1H, amid NH), 11.17 (s, 1H, aryl–OH), 11.58 (s, 1H, aryl–OH). ^{13}C NMR (62.90 MHz, DMSO-d^6, ppm) (ismer I + isomer II): + 25.04 (–CH_2–), 34.19 + 34.22 (CH_2CO–), 110.79 + 110.81, 118.80 + 119.02, 121.63 + 123.08, 130.93 + 133.76, 138.88, 144.40 (–CH=N–), 155.88 + 156.71, 168.94 (–CO–). UV–Vis spectrum in CH_3OH [λ_{max} (ε, $dm^3\ mol^{-1}\ cm^{-1}$)]: 227 (44,000), 282 (49,300), 334 nm (22,500).

(N’^{1}E,N’^{6}E)–N’^{1},N’^{6}-bis(2-hydroxy-3-methoxybenzylidene)adipohydrazide (H_4L^3)

Yield: 91%. Anal. Calc. for $C_{22}H_{26}N_4O_6$ (MW 442.47): C, 59.7; H, 5.9; N, 12.7. Found: C, 59.7; H, 5.9; N, 12.7. IR (KBr, cm^{-1}): 3,454 (s, O–H), 3,215 (m, N–H), 3,083 (w), 2,943 (m), 2,863 (w), 1,668 (vs, C=O), 1,631 (m), 1,579 (w), 1,471 (m), 1,412 (m), 1,254 (vs, phenolic O–H), 1,153 (w), 1,081 (m), 973 (w), 777 (w), 731 (m), 563 (w). ^1H NMR (250.13 MHz, DMSO-d^6, ppm): 1.60 (m, 4H, CH_2), 2.22 (m, 2H, –CO–CH_2), 2.58 (m, 2H, CO–CH_2), 3.70 (s, 6H, OCH_3), 6.80–7.2 (m, 6 H, aryl), 8.20 (s, 1H, CH=N), 8.30 (s, 1H, CH=N), 9.48 (s, 1 H, N–H), 10.86 (s, 1H, N–H), 11.15 (s, 1H, O–H), 11.50 (s, 1H, O–H). ^{13}C NMR (62.90 MHz, DMSO-d^6, ppm) (ismer I + isomer II): 25.03 + 25.10 (–CH_2–), 32.15 + 34.16 (CH_2CO–), 56.21 (CH_3), 113.27 + 114.11, 118.67 + 119.15, 119.48 + 119.52, 146.32 (–CH=N–), 147.01, 147.36, 148.26 + 148. 36, 174.38 + 168.99 (–CO–).

UV–Vis spectrum in CH_3OH [λ_{max} (ε, dm^3 mol^{-1} cm^{-1})]: 205 (30,800), 230 (29,800), 290 (37,100), 331 nm (11,400).

Synthesis of [{$VO(CH_3OH)(OCH_3)$}$_2L^{1-3}$] (1–3)

These complexes were synthesized by the same general method as follows: the appropriate ligand (H_4L^1, H_4L^2, or H_4L^3) (0.27 mmol) was dissolved in methanol (10 mL), [$VO(acac)_2$] (0.54 mmol) was added, and the solution was gently refluxed for 4 h. After cooling, the resulting solid was filtered off, washed with methanol, and dried in air.

For the preparation of suitable single crystals for X-ray analysis, the appropriate ligand (H_4L^1 or H_4L^3) (0.027 mmol) and $VO(acac)_2$ (0.054 mmol) were placed in the main arm of a branched tube (‘branched tube’ method). A mixture of methanol and acetonitrile (15:85 v/v, 15 mL) was carefully added to fill the arms, the tube was sealed, and reagents containing arm immersed in an oil bath at 60 °C while the other arm was kept at ambient temperature. After week, dark brown crystals that were suitable for X-ray analysis were deposited in the cooler arm, which were filtered off, washed with methanol, and dried in air.

[{$VO(CH_3OH)(OCH_3)$}$_2L^1$] (**1**)

Yield: 72%. Anal. Calc. for $C_{32}H_{36}N_4O_{10}V_2$ (MW 738.53): C, 52.0; H, 4.9; N, 7.6; V, 13.8. Found: C, 51.9; H, 4.9; N, 7.6; V, 14.0. IR (KBr, cm^{-1}): 3,466 (m, O–H), 3,073 (w), 2,957 (m), 2,810 (w), 1,602 (vs, C=N–N=C), 1,557(s), 1,451 (m), 1,391 (m), 1,332 (s), 1,303 (s), 1,200 (s), 1,148 (m), 1,048 (s), 994 (s, V=O), 832 (m), 756 (m), 631 (s), 596 (m), 520 (w). ^1H NMR (250.13 MHz, DMSO-d^6, ppm): 1.41 (m, 2H, CH_2), 1.73 (m, 4H, CH_2 and CH_2–CO), 2.05 (m, 2H, CO–CH_2), 3.15 (s, 12 H, methoxy), 7.08–8.42 (m, 12H, aryl), 9.60 (s, 2 H, CH=N).

[{$VO(CH_3OH)(OCH_3)$}$_2L^2$] (**2**)

Yield: 74%. Anal. Calc. for $C_{24}H_{30}Br_2N_4O_{10}V_2$ (MW 796.21): C, 36.2; H, 3.8; N, 7.0; V, 12.8. Found: C, 36.2; H, 3.8; N, 7.1; V, 12.5. IR (KBr, cm^{-1}): 3,443 (s, vbr, O–H), 3,091 (w), 2,944 (m), 2,868 (w), 2,811 (w), 1,617 (vs, C=N–N=C), 1,547 (vs), 1,461 (s), 1,415 (m), 1,377 (m), 1,352 (m), 1,279 (s), 1,197 (m), 1,140 (w), 1,056 (m), 1,007 (m), 983 (m), 921 (w), 826 (s), 786 (w), 711 (m), 668 (m), 629 (m), 574 (m), 475 (m).

[{$VO(CH_3OH)(OCH_3)$}$_2L^3$]·$2CH_3OH$ (**3**)

Yield: 73%. Anal. Calc. for $C_{28}H_{44}N_4O_{12}V_2$ (MW 762.55): C, 44.1; H, 5.8; N, 7.4; V, 13.4. Found: C, 44.2; H, 5.9; N, 7.3; V, 13.5. IR (KBr, cm^{-1}): 3,457 (s,vbr), 3,071 (w), 2,937 (m), 2,841 (w), 1,610 (vs, C=N–N=C), 1,564 (vs), 1,470 (m), 1,438 (s), 1,353 (m), 1,259 (vs), 1,226 (m), 1,108 (m), 1,088 (m), 999 (s), 963 (s), 876 (m), 786 (s) 741 (vs), 620 (m), 472 (w).

X-ray structure determination

Single crystals of **1** and **3** were carefully selected under a polarizing microscope. Dark brown crystals of **1** (0.12 mm × 0.06 mm × 0.05 mm) and **3** (0.20 mm × 0.17 mm × 0.10 mm) were investigated in diffraction experiments at 173 (2) K on an Oxford XCalibur diffractometer with monochromated Mo–$K\alpha$ radiation (λ = 0.71073 Å). Crystallographic data and data collection parameters are given in Table 9. The structures were

Table 9 Crystal data and structure refinement for [{$VO(CH_3OH)(OCH_3)$}$_2L^1$] (**1**) and [{$VO(CH_3OH)(OCH_3)$}$_2L^3$]·$2CH_3OH$ (**3**)

Complex	1	3
Net formula	$C_{32}H_{36}N_4O_{10}V_2$	$C_{28}H_{44}N_4O_{14}V_2$
M_r/g mol^{-1}	738.532	762.551
Crystal system	Triclinic	Monoclinic
Space group	*P*1 bar	$P2_1/c$
a/Å	9.5393(7)	13.6334(7)
b/Å	10.6862(6)	9.2255(4)
c/Å	17.3371(11)	13.4991(7)
α/°	79.098(5)	90
β/°	85.175(5)	101.249(5)
γ/°	68.961(6)	90
V/Å^3	1,619.48(18)	1,665.23(14)
Z	2	2
Calc. density/g cm^{-3}	1.51453(17)	1.52083(13)
μ/mm^{-1}	0.641	0.634
Absorption correction	‘Multi-scan’	‘Multi-scan’
Transmission factor range	0.99240–1.00000	0.97681–1.00000
Refls. measured	11537	7,063
R_{int}	0.0759	0.0415
Mean $\sigma(I)/I$	0.2708	0.0787
θ range	4.14–25.24	4.29–26.32
Observed refls.	2,257	2,227
x, y (weighting scheme)	0, 0	0.0549, 0
Hydrogen refinement	Mixed	Constr.
Refls in refinement	5,834	3,388
Parameters	443	221
Restraints	2	0
$R(F_{obs})$	0.0487	0.0457
$R_w(F^2)$	0.0560	0.1134
S	0.652	0.938
Shift/error$_{max}$	0.001	0.001
Max electron density/e Å^{-3}	0.398	0.894
Min electron density/e Å^{-3}	−0.364	−0.564

solved by direct methods with SIR97 [31] and refined with full-matrix least-squares techniques on F^2 with SHELXL-97 [32]. In **1**, C-bound H was constrained to ride on their parent atoms, and O-bound H was fixed to a distance of 0.82(2) Å with $U(H) = 1.5\ U(O)$. Graphics were drawn with DIAMOND [33] and MERCURY.

General oxidation procedure

The liquid-phase catalytic oxidations were carried out under air (atmospheric pressure) in a 25-mL round-bottom flask equipped with a magnetic stirrer and immersed in a thermostated oil bath at 80 ± 1 °C. In a typical experiment, a mixture of H_2O_2 (3 mmol), solvent (3 mL), chlorobenzene (0.1 g), and cyclooctene (1 mmol) was added to a flask containing the catalyst **1**, **2**, or **3** (about 1.3 μmol). The course of the reaction was monitored using a gas chromatograph equipped with a capillary column and a flame ionization detector. The oxidation products were identified by comparing their retention times with those of authentic samples or alternatively by ^{1}H NMR. In some instances, reactions were carried out on a larger scale and the epoxides were isolated as further confirmation of identity and yield by NMR. Substrate conversion (%) and oxidation product yields based on the starting substrate were quantified by comparison with internal standard chlorobenzene. Control reactions were carried out in the absence of catalyst (under the same conditions as the catalytic runs) and H_2O_2. No products were detected or yields were trace.

Supplementary data

Crystallographic data (excluding structure factors) have been deposited at the Cambridge Crystallographic Data Center (CCDC) as Supplementary Publication CCDC-826012 and 826013 for **1** and **3**, respectively. Copies of the data can be obtained free of charge on application to the CCDC, 12 Union Road, Cambridge, CB2 1EZ, UK (fax: +44 1223-336-033; e-mail: deposit@ccdc.cam.ac.uk).

Acknowledgments The authors are grateful to the Zanjan University, the Faculty of Chemistry and Biochemistry of the Ludwig-Maximilians-Universität München, and the School of Chemistry for financial assistance.

References

1. Mohan M, Gupta MP, Chandra L, Jha NK (1988) Inorg Chim Acta 151:61–68
2. Richardson DR, Ponka P (1988) Am J Hematol 58:299–305
3. Kalinowski DS, Sharpe PC, Bernhardt PV, Richardson DR (2008) J Med Chem 51:331–344
4. Bernhardt PV, Chin P, Sharpe PC, Wang JYC, Richardson DR (2005) J Biol Inorg Chem 10:761–777
5. Tamasi G, Chiasserini L, Savini L, Sega A, Cini R (2005) J Inorg Biochem 99:1347–1359
6. Bakir M, Hassan I, Johnson T, Brown O, Green O, Gyles C, Coley MD (2004) J Mol Struct 688:213–222
7. Ward MD (2005) J Solid State Electrochem 9:778–787
8. Desjardins YQP, Wang ZY (2002) J Optics A 4:S273–S277
9. Stadler AM, Harrowfield J (2009) Inorg Chim Acta 362:4298–4314
10. Pouralimardan O, Chamayou AC, Janiak C, Hosseini Monfared H (2007) Inorg Chim Acta 360:1599–1608
11. Adams H, Fenton DE, Minardi G, Mura E, Pistuddi AM, Solinas C (2000) Inorg Chem Commun 3:24–28
12. Larin GM, Minin VV, Shul'gin VF (2008) Russ Chem Rev 77:451–465
13. Eady RR (2003) Coord Chem Rev 237:23–30
14. Carter-Franklin JN, Parrish JD, Tchirret-Guth RA, Little RD, Butler A (2003) J Am Chem Soc 125(13):3688–3689
15. Crans DC, Mahroof-Tahir M, Shin PK, Keramidas AD (1995) Mol Cell Biochem 153:17–24
16. Antipov AA, Sorokin DY, L'Vov NP, Kuenen JG (2003) Biochem J 369:185–189
17. Plass W (1999) Angew Chem Int Ed Engl 38:909–912
18. Nica S, Pohlmann A, Plass W (2005) Eur J Inorg Chem 8:2032–2036
19. Ghosh T (2006) Transit Met Chem 31:560–563
20. Battistel E, Tassinari R, Fornaroli M, Bonoldi L (2003) J Mol Catal A Chem 202:107–115
21. Shulpin GB, Atanasio D, Suber L (1993) J Catal 142:147–152
22. Si TK, Chowdhury K, Mukherjee M, Bera DC, Bhattacharyya R (2004) J Mol Catal A Chem 219:241–247
23. Larin GM, Shul′gin VF, Gusev AN, Cherneg AN (2004) Russ Chem Bull 53:775–779
24. Kolawole G, Patel KS (1981) J Chem Soc Dalton Trans 1241–1245
25. Moon M, Pyo M, Myoung YC, Ahn CI, Lah MS (2001) Inorg Chem 40:554–557
26. Cotton FA, Wilkinson G (1988) Advanced inorganic chemistry, 5th edn. Wiley, New York, p 458
27. Huheey JE (1983) Inorganic chemistry: principles of structure and reactivity, 3rd edn. Harper and Row Publisher Inc, New York, p 340
28. Appleton AJ, Evans S, Lindsay Smith JR (1996) J Chem Soc Perkin Trans 2:281–285
29. Hosseini Monfared H, Bikas R, Mayer P (2010) Inorg Chim Acta 363:2574–2583
30. Hosseini Monfared H, Kheirabadi S, Asghari Lalami N, Mayer P (2011) Polyhedron 30:1375–1384
31. Altomare A, Burla MC, Camalli M, Cascarano GL, Giacovazzo C, Guagliardi A, Moliterni AGG, Polidori G (1999) Appl Crystallogr 32:115–119
32. Sheldrick GM (2008) Acta Crystallogr A64:112–122
33. DIAMOND (version 3.0) for Windows. Crystal Impact Gbr, Bonn, Germany, 2004. Available from: http://www.crystalimpact.com/diamond